Kinematic analysis of a 6R single-loop overconstrained spatial mechanism for circular translation

Kinematic Analysis of a 6R Single-loop Overconstrained Spatial Mechanism for Circular Translation

Xianwen Kong

School of Engineering and Physical Sciences
Heriot-Watt University
Edinburgh, UK, EH14 4AS
Email: X.Kong@hw.ac.uk
Tel: +44(0)1314513688

Abstract

This paper deals with the kinematic analysis of a double-spherical 6R and parallelogram 4R based single-degree-of-freedom overconstrained 6R spatial mechanism for circular translation (DSPB6RCT). How to construct a DSPB6RCT is recalled first. A closed-form solution to the kinematic analysis of the mechanism is then discussed in detail. The kinematic analysis of the mechanism is reduced to the solution of a univariate quadratic equation. The self-motion of a DSPB6RCT is further investigated. The analysis shows that a DSPB6RCT usually has two solutions to the kinematic analysis for a given input. Numerical examples show that this class of mechanisms may have 0, 2 or 4 full-turn revolute joints and one or two circuits (closure modes or branches). This work provides a solid starting point for further investigation on the classification and application of DSPB6RCTs as well as the kinematic analysis of other classes of overconstrained 6R spatial mechanisms for circular translation. The results can also be used for the type synthesis and singularity analysis of translational parallel mechanisms.

Keywords:
Overconstrained Mechanism, Kinematic Analysis, Parallelogram, Self-motion, Parallel Mechanism

1. Introduction

A single-loop system composed of $m(m \leq 6)$-links connected by m single degree-of-freedom (DOF) joints is usually a structure and can be a 1-DOF

overconstrained single-loop mechanism under specific geometric conditions. The research on single DOF single-loop overconstrained mechanisms started from 1853 when the Sarrus mechanism appeared. Since then, a number of single-loop overconstrained spatial mechanisms [1, 2, 3, 4, 5, 6, 7, 8, 9, 10, 11, 12, 13, 14, 15, 16] have been proposed. Meanwhile, different approaches, such as construction approaches [1, 5, 9, 16], geometric methods [12], algebraic approaches [3, 8, 10, 11, 14, 15, 17, 19, 21, 22] and numerical methods [4, 13, 23], have been developed to the synthesis and analysis of overconstrained mechanisms. Searching for overconstrained mechanisms is challenging. Even the four-link overconstrained mechanisms had not been identified completely until 2011 [12], let alone the five- and six-link overconstrained mechanisms.

Although the successful industrial applications of single-loop overconstrained mechanisms are not many so far, the potential application of single-loop overconstrained mechanisms in deployable structures [9, 23], disassembly-free reconfigurable single-loop mechanisms [24, 25, 26, 27, 28, 29], parallel mechanisms [30], disassembly-free reconfigurable parallel mechanisms [31, 32] and other devices [33] is being explored.

Recently, the author of this paper obtained six 6R overconstrained single-loop spatial mechanisms for circular translation [16], which focuses on how to obtain the 6R overconstrained spatial mechanisms for circular translation using a construction method without algebraic derivation and detailed kinematic analysis of DSPB6RCTs. Here and throughout this paper, R denotes a revolute joint. These mechanisms not only provide potential alternatives to the widely-used planar parallelograms, but also can be used for the type synthesis and singularity analysis of translational parallel mechanisms [35].

Among the six 6R overconstrained spatial mechanisms for circular translation, four mechanisms have two pairs of adjacent R joints with parallel axes and one pair of non-adjacent R joints with parallel axes. Mechanisms with three pairs of R joints with parallel axes are called parallel 6R mechanisms in [15], where three types of parallel 6R mechanisms have been obtained independently using a dual quaternion approach. Unlike the construction approach [16] in which the design objective is the circular translation between a pair of links, the design objective of the dual quaternion approach [15] is only the DOF of the 6R overconstrained mechanism. It is noted that a special case of parallel 6R mechanisms was first proposed in [6, 7], which had been unfortunately ignored by researchers working on overconstrained 6R mechanisms for more than a decade [14, 15, 16, 18]. In [6, 7, 14, 15], it was not revealed that two pairs of links undergo circular translation with

respect to each other.

The double-spherical 6R and parallelogram 4R based single-degree-of-freedom overconstrained 6R spatial mechanism for circular translation (DSPB6RCT), which will be described in Section 2, has a simple kinematic structure and may have application potentials. During the revision of this paper, the author noticed the publication of [34] in which a geometric approach was proposed to construct the DSPB6RCT. Using the method in [34], certain geometric insight can be revealed. However, one more planar parallelogram is needed for constructing a DSPB6RCT in [34] than in [16]. In addition, five types of 6R mechanisms for circular translation cannot be obtained using the approach in [34] in its current state. At present, the in-depth kinematic analysis of DSPB6RCTs is still not available.

This paper aims at deriving the solutions to kinematic analysis of the DSPB6RCTs and revealing the kinematic characteristics and conditions for self-motion [37, 38] of the DSPB6RCT.

This paper is organized as follows. A description of the DSPB6RCT is given in Section 2. Section 3 deals with the overconstraint analysis of the DSPB6RCT. The kinematic analysis of the DSPB6RCT is presented in detail in Section 4. Section 5 deals with the self-motion analysis of DSPB6RCTs. Several numerical examples of DSPB6RCTs with different number of full-turn R joints and different number of circuits (closure modes or branches) are given in Section 6. Finally, conclusions are drawn.

For simplicity reasons, $\sin\alpha_i$, $\cos\alpha_i$, $\sin\theta_i$ and $\cos\theta_i$ are denoted by $S\alpha_i$, $C\alpha_i$, $S\theta_i$ and $C\theta_i$, respectively.

2. Description of a DSPB6RCT

In this section, the construction of a DSPB6RCT [16] is recalled first. The coordinates frames are then set up on the links of the mechanism to define link parameters of the mechanism.

2.1. Construction of a DSPB6RCT

According to [16], a DSPB6RCT can be constructed in three steps.

First, obtain a double-spherical 6R overconstrained spatial mechanism for circular translation from a general one-DOF double-spherical 6R overconstrained spatial mechanism [1] by imposing certain constraints. Figure 1(a) shows a double-spherical 6R overconstrained spatial mechanism for circular translation, in which the axes of joints 1, 2 and 3 meet at one point and

those of joints 4, 5 and 6 meet at another point. In Fig. 1 and throughout this paper, a small sphere represents the intersection of joint axes of R joints of the same link. There are three pairs of joints with parallel axes: joints 6 and 1, joints 2 and 5, as well as joints 3 and 4. Using screw theory (see [35] for example), we can prove that links I and II undergo circular translation with respect to links V and IV respectively. In the following, it will be proved that link I undergoes circular translation with respect to link V.

In a given configuration, there are three pairs of joints with parallel axes: joints 6 and 1, joints 2 and 5, as well as joints 3 and 4. Therefore, Link V imposes one constraint couple, whose direction is perpendicular to the axes of joints 2, 3, 4 and 5, through sub-chain 2-3-4-5 and two independent constraint couples, whose directions are perpendicular to the axes of joints 6 and 1, through sub-chain 6-1 on link I. These three constraint couples are generally not coplanar and therefore independent. Thus link I can only translate with respect to link V. Under the action of further constraint forces by Link VI, on which joints 6 and 1 have parallel axes and the distance between the axes of joints 6 and 1 is constant, Link I undergoes circular translation with respect to link V in this configuration. If link I moves to a new position from the given configuration, there are still three pairs of joints with parallel axes: joints 6 and 1, joints 2 and 5, as well as joints 3 and 4. Based on the above analysis, link I can still only undergo circular translation with respect to link V in the new configuration. Therefore, link I undergoes circular translation with respect to link V.

Since links I and II undergo circular translation with respect to links V and IV respectively, we can then connect link I to link V using link VI' and link II to link IV using link III' respectively without affecting the motion of the mechanism (Fig. 1(b)). Here, link VI' forms one planar parallelogram with links I, V and VI, and link III' forms another planar parallelogram with links II, IV and III. In this way, we obtain a single-DOF 2R-2Parallelogram mechanism composed of two planar parallelograms and two R joints.

Finally, by removing links III and VI from the 2R-2Parallelogram mechanism shown in Fig. 1(b), we can obtain a general DSPB6RCT (Fig. 1(c)), in which links I and II undergo circular translation with respect to links V and IV respectively.

2.2. Link parameters of a DSPB6RCT

Considering that different variations of D-H notations are used in the literature [5, 8, 9, 19, 25], we first clarify how the coordinate frames are

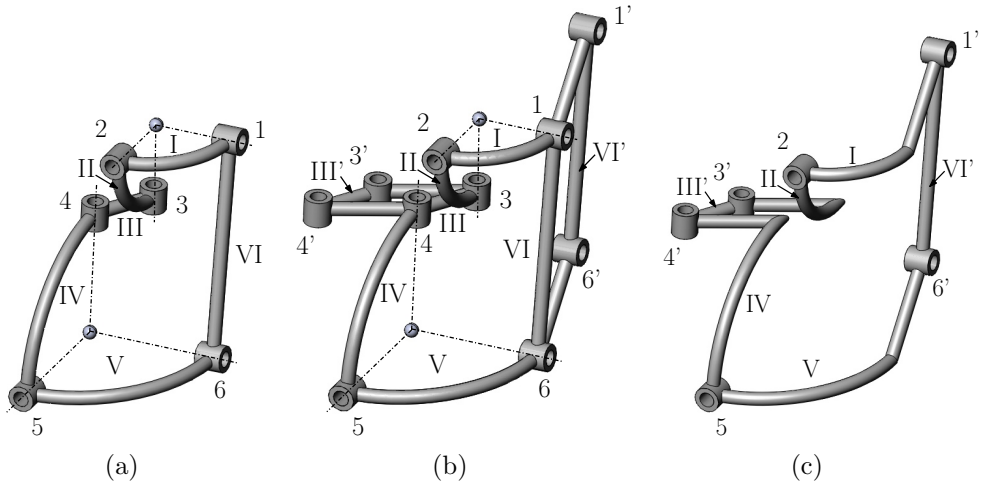

Figure 1: Construction of a DSPB6RCT: (a) Double-spherical 6R mechanism for circular translation; (b) 2R-2Parallelogram mechanism for circular translation; (c) DSPB6RCT.

attached to the links and the link parameters are defined in this paper. As shown in Fig. 2, coordinate frames are attached to the links in the mechanism as follows: Z_i-axis is along the axis of joint i. X_i-axis is along the common perpendicular between Z_{i-1}- and Z_i-axes. O_i is the intersection of X_i- and Z_i-axes. Y_i-axis is defined by X_i- and Z_i-axes through the right handed rule. The link parameters of link i are: d_i (the distance between X_i- and X_{i+1}-axes measured from X_i-axis to X_{i+1}- axis along Z_i-axis), α_i (the twist angle between Z_i- and Z_{i+1} axes measured from Z_i-axis to Z_{i+1}-axis about X_{i+1}-axis), and l_i (the distance between Z_i- and Z_{i+1}-axes measured from Z_i-axis to Z_{i+1}-axis along X_{i+1}-axis).[1] The joint variable of joint i is denoted by θ_i (the angle between X_i- and X_{i+1}-axes measured from X_i-axis to X_{i+1} axis about Z_i-axis). It is noted that both d_i and l_i are within the range of $(-\infty, \infty)$ in this paper, although it is common to limit l_i within the range of $[0, \infty)$. In this way, we can create coordinate axes along parallel joint axes with the same positive direction in order to make the representation of the constraints on the link parameters simple (see Eq. (1) later in this section).

There are usually different sets of D-H link parameters for a given mechanism due to the different coordinate frames used [36]. How to detect rapidly

[1]It is noted that l_i in this paper is denoted by a_i in [25, 19], a_{i+1} in [5], and $a_{i(i+1)}$ in [8, 9], respectively.

whether different sets of D-H link parameters represent the same mechanism deserves further investigation.

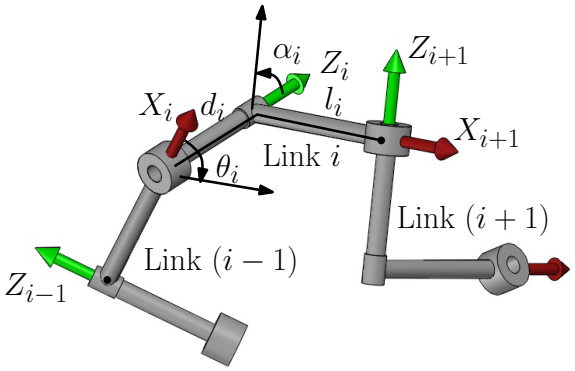

Figure 2: D-H notation.

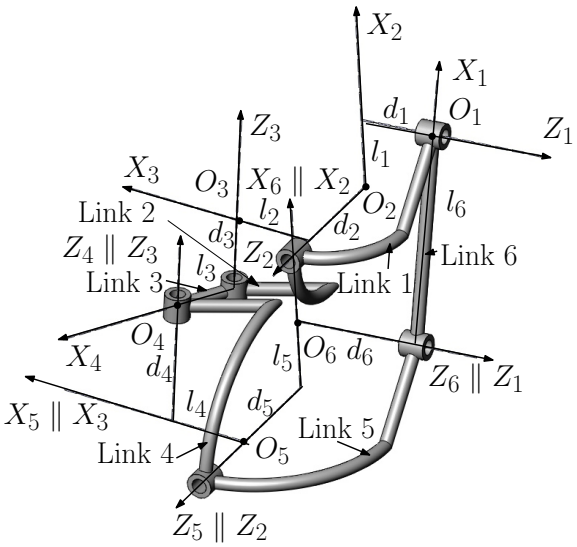

Figure 3: Coordinate frames of a DSPB6RCT.

A DSPB6RCT is shown in Fig. 3 [16]. In this mechanism, two links (links 6 and 3) have two R joints with parallel axes. The axes of the remaining two R joints are also parallel to each other during the motion of the mechanism. Links 1 and 2 undergo circular translation with respect to links 5 and 4, respectively. Let the positive directions of the coordinate axes that

are parallel, including Z_6- and Z_1-axes, Z_3- and Z_4-axes, Z_2- and Z_5-axes, X_2- and X_6-axes as well as X_3- and X_5-axes, be along the same direction. The link parameters of the DSPB6RCT satisfy

$$\begin{cases} \alpha_3 = 0 \\ \alpha_6 = 0 \\ \alpha_4 = -\alpha_2 \\ \alpha_5 = -\alpha_1 \\ l_5 = -l_1 \\ l_4 = -l_2 \\ d_5 = -d_2 \end{cases} \tag{1}$$

During the motion of the DSPB6RCT, the pairs of parallel coordinate axes remain parallel. Since the parallel coordinate axes are along the same positive direction, we have

$$\begin{cases} \theta_6 = -\theta_1 \\ \theta_5 = -\theta_2 \\ \theta_4 = -\theta_3 \end{cases} \tag{2}$$

Although the conditions on the link parameters that the DSPB6RCT satisfy have been shown in the construction of the mechanism in Section 2.1[16], the algebraic existence criteria, except for those in Eq. (1), that the DSPB6RCT must satisfy are not apparent and should be derived. Such conditions, called closure condition in the literature (see [19] for example), ensure the redundant kinematic equations are compatible and have solutions. Like in the cases of Bricard's trihedral mechanisms [19] and the double-spherical 6R overconstrained mechanisms [20, 21], a closure condition usually involves link parameters of at least three links of a 6R overconstrained spatial mechanism.

3. Overconstraint analysis of the DSPB6RCT

3.1. Kinematic equations of a 6R overconstrained mechanism

To derive the closure condition of the DSPB6RCT and closed-form solution to the kinematic analysis, we will first set up the kinematic equation of the 6R overconstrained spatial mechanism. Different approaches have been proposed for the kinematic analysis of the 6R overconstrained mechanisms [2, 3, 4, 5, 6, 7, 8, 9, 10, 11, 12, 13, 14, 17]. A matrix based method (see [17]

for example) will be used in this paper for the analysis of 6R overconstrained mechanisms.

The homogeneous transformation matrix T_i of O_{i+1}-$X_{i+1}Y_{i+1}Z_{i+1}$ with respect to O_i-$X_iY_iZ_i$ (Fig. 2) is

$$T_i = \begin{bmatrix} C\theta_i & -S\theta_i C\alpha_i & S\theta_i S\alpha_i & C\theta_i l_i \\ S\theta_i & C\theta_i C\alpha_i & -C\theta_i S\alpha_i & S\theta_i l_i \\ 0 & S\alpha_i & C\alpha_i & d_i \\ 0 & 0 & 0 & 1 \end{bmatrix} \tag{3}$$

The inverse of T_i, which represents the homogeneous transformation matrix of O_i-$X_iY_iZ_i$ with respect to O_{i+1}-$X_{i+1}Y_{i+1}Z_{i+1}$, is

$$T_i^{-1} = \begin{bmatrix} C\theta_i & S\theta_i & 0 & -l_i \\ -S\theta_i C\alpha_i & C\theta_i C\alpha_i & S\alpha_i & -S\alpha_i d_i \\ S\theta_i S\alpha_i & -C\theta_i S\alpha_i & C\alpha_i & -C\alpha_i d_i \\ 0 & 0 & 0 & 1 \end{bmatrix} \tag{4}$$

Using the homogeneous transformation matrix (Eq. (3)), the closed-loop kinematic equation of the 6R overconstrained mechanism is

$$T_1 T_2 T_3 T_4 T_5 T_6 = I \tag{5}$$

where I is the 4×4 identity matrix.
Multiplying Eq.(5) using T_1^{-1} from the left and $T_6^{-1}T_5^{-1}$ from the right, we have

$$T_2 T_3 T_4 = T_1^{-1} T_6^{-1} T_5^{-1} \tag{6}$$

It is noted that several equations similar to Eq. (6), such as $T_1T_2T_3 = T_6^{-1}T_5^{-1}T_4^{-1}$[17], can be obtained from Eq. (5). The left-hand side of Eq. (6) is associated with kinematic chain 2-3-4 in which joints 3 and 4 have parallel joint axes, and the right-hand side of Eq. (6) is associated with kinematic chain 5-6-1 in which joints 6 and 1 have parallel joint axes. From Eq. (2), we learn that each side of Eq. (6) involves two joint variables, whereas there are three joint variables in each side of equations like $T_1T_2T_3 = T_6^{-1}T_5^{-1}T_4^{-1}$. Equation (6) will be used in this paper since it will lead to a more concise solution to the kinematic analysis of a DSPB6RCT.

3.2. Kinematic equations of a DSPB6RCT

Substituting Eqs. (1)–(4) into Eq. (6), we have

$$\begin{bmatrix} C\theta_2 & -S\theta_2 & 0 & f_{1a} \\ S\theta_2 & C\theta_2 & 0 & f_{2a} \\ 0 & 0 & 1 & f_{3a} \\ 0 & 0 & 0 & 1 \end{bmatrix} = \begin{bmatrix} C\theta_2 & -S\theta_2 & 0 & f_{1b} \\ S\theta_2 & C\theta_2 & 0 & f_{2b} \\ 0 & 0 & 1 & f_{3b} \\ 0 & 0 & 0 & 1 \end{bmatrix} \tag{7}$$

where

$$\begin{aligned} f_{1a} &= S\theta_2 S\alpha_2(d_3+d_4) + C\theta_2 C\theta_3 l_3 - S\theta_2 C\alpha_2 S\theta_3 l_3 \\ f_{2a} &= -C\theta_2 S\alpha_2(d_3+d_4) + S\theta_2 C\theta_3 l_3 + C\theta_2 C\alpha_2 S\theta_3 l_3 \\ f_{3a} &= C\alpha_2(d_3+d_4) + S\alpha_2 S\theta_3 l_3 + d_2 \\ f_{1b} &= -C\theta_1 l_6 \\ f_{2b} &= S\theta_1 C\alpha_1 l_6 - S\alpha_1(d_6+d_1) \\ f_{3b} &= d_2 - S\theta_1 S\alpha_1 l_6 - C\alpha_1(d_6+d_1) \end{aligned}$$

i.e.

$$\begin{bmatrix} 0 & 0 & 0 & f_{1a}-f_{1b} \\ 0 & 0 & 0 & f_{2a}-f_{2b} \\ 0 & 0 & 0 & f_{3a}-f_{3b} \\ 0 & 0 & 0 & 0 \end{bmatrix} = 0 \tag{8}$$

Equation (8) is in fact the following set of three equations.

$$\begin{cases} f_{1a}-f_{1b}=0 \\ f_{2a}-f_{2b}=0 \\ f_{3a}-f_{3b}=0 \end{cases} \tag{9}$$

Equation (9) will be used for identifying the closure condition of the DSPB6RCT in Section 3.3 and for deriving the closed-form solution to the kinematic analysis in Section 4 and the self-motion analysis in Section 5.

3.3. Closure condition of a DSPB6RCT

In Eq. (9), there are three equations in three variables θ_1, θ_2 and θ_3. Since the DSPB6RCT has one DOF, two out of the three variables are dependent. Therefore, the three equations in Eq. (9) are also dependent. To ensure the three equations are compatible and have solutions, the link parameters of

the DSPB6RCT must satisfy a closure condition, which will be derived in the following.

Equation (9) can be rewritten as

$$\begin{cases} f_{1a} = f_{1b} \\ f_{2a} = f_{2b} \\ f_{3a} - d_2 = f_{3b} - d_2 \end{cases} \tag{10}$$

Taking the sum of the squares of both sides of the three equations in Eq. (10), we have

$$f_{1a}^2 + f_{2a}^2 + (f_{3a} - d_2)^2 = f_{1b}^2 + f_{2b}^2 + (f_{3b} - d_2)^2$$

i.e.

$$(d_3 + d_4)^2 + l_3^2 = (d_1 + d_6)^2 + l_6^2 \tag{11}$$

Equation (11) is the closure condition of the DSPB6RCT. It involves link parameters of three links including links 3, 4 and 6. It is noted that since joints 1 and 6 and joints 3 and 4 have parallel joint axes respectively, one of d_3 and d_4 and one of d_1 and d_6 can be set to 0.

Equations (1) and (11) are the existence criteria of the DSPB6RCT. These criteria are equivalent to those for the parallel 6R mechanisms with translational property identified in [15]. This confirms that the DSPB6RCT and the parallel 6R mechanisms with translational property are the same mechanism. Unlike the R-X-X-R mechanism [20], two pairs of joints with intersecting joint axes are not compulsory for DSPB6RCTs.

4. Kinematic analysis of the DSPB6RCT

For a DSPB6RCT, we have Eqs. (1) and (11). The three equations in Eq. (9) are non-linearly dependent. One can obtain the two dependent variables (outputs) for a given input by solving Eq. (9). Let θ_3 be the input of the DSPB6RCT and θ_1 and θ_2 denote the outputs.

Rewriting the third equation of Eq. (9) in $S\theta_1$ and $C\theta_1$, we have

$$C_{11} S\theta_1 + C_{13} = 0 \tag{12}$$

where

$$\begin{aligned} C_{11} &= S\alpha_1 l_6 \\ C_{13} &= C\alpha_2(d_3 + d_4) + S\alpha_2 S\theta_3 l_3 + C\alpha_1(d_6 + d_1) \end{aligned}$$

As well-documented in the literature, for a given θ_3, we can obtain up to two solutions to θ_1 using Eq. (12).

The first two equations in Eq. (9) can be rewritten in the form of a set of two linear equations in $S\theta_2$ and $C\theta_2$ as

$$\begin{cases} A_{11}S\theta_2 + A_{12}C\theta_2 + A_{13} = 0 \\ A_{21}S\theta_2 + A_{22}C\theta_2 + A_{23} = 0 \end{cases} \tag{13}$$

where

$$\begin{aligned} A_{11} &= S\alpha_2(d_3 + d_4) - S\theta_3 C\alpha_2 l_3 \\ A_{12} &= l_3 C\theta_3 \\ A_{13} &= l_6 C\theta_1 \\ A_{21} &= A_{12} \\ A_{22} &= -A_{11} \\ A_{23} &= S\alpha_1(d_6 + d_1) - S\theta_1 C\alpha_1 l_6 \end{aligned}$$

Solving Eq. (13), we have

$$\begin{cases} S\theta_2 = (-A_{13}A_{22} + A_{23}A_{12})/D \\ C\theta_2 = (-A_{23}A_{11} + A_{13}A_{21})/D \end{cases} \tag{14}$$

where $D = A_{11}A_{22} - A_{21}A_{12}$.

For a given set of θ_3 and θ_1, we can obtain one solution to $S\theta_2$ and $C\theta_2$ (Eq. (14)) and therefore one solution to θ_2. The closure condition (Eq. (11)) guarantees that the solution to $S\theta_2$ and $C\theta_2$ satisfies $S^2\theta_2 + C^2\theta_2 = 1$. Then a set of θ_4, θ_5 and θ_6 can be obtained using Eq. (2) for each set of θ_1, θ_2 and θ_3.

The above analysis shows that for a given input θ_3, there are generally two sets of solutions (Eqs. (12), (14) and (2)) to the kinematic analysis of the DSPB6RCT. It is noted that the solutions to the kinematic analysis of this mechanism is independent of link parameters d_2, $d_5(= -d_2)$, l_1, l_2, $l_4(= -l_2)$ and $l_5(= -l_1)$.

It can be verified through numerical examples that a general 6R mechanism satisfying the existence criteria (Eqs. (1) and (11)) usually undergoes only motion satisfying Eq. (2). There may exist solutions associated with 6R structures for certain sets of link parameters. The structures are excluded from the solutions and the determination of such structures are out of the scope of this paper.

It is noted that the mechanism in Fig. 1(a) can be regarded as both a DSPB6RCT with $l_1 = l_2 = d_2 = 0$ and a special case of the double-spherical 6R overconstrained mechanism. Since there are usually four solutions to the kinematic analysis of a double-spherical 6R overconstrained mechanism [20, 21], the mechanism in Fig. 1(a) can also undergo motion not satisfying Eq. (2). It is still open to identify DSPB6RCTs that also satisfy the existence criteria of other classes of 6R overconstrained spatial mechanisms, which may also undergo motion not satisfying Eq. (2), as potential disassembly-free reconfigurable mechanisms.

5. Self-motion analysis of DSPB6RCTs

Like some parallel mechanisms which may undergo self-motion [37, 38], which refers to the finite motion of some links of a mechanism when all the actuated joints are locked, certain DSPB6RCT may also undergo self-motion when the actuated joint, joint 3, is locked. The condition for self-motion of a mechanism can be derived by considering the special cases encountered in the displacement analysis of a mechanism [38]. This section will deal with the self-motion analysis of DSPB6RCTs.

Equation (14) holds if $D \neq 0$. If $D = 0$ and Eq. (9) has solutions, then θ_2 can be of any value, and the DSPB6RCT undergoes self-motion. The self-motion analysis of DSPB6RCTs can be carried out as follows.

Substituting A_{ij} (i=1 and 2, j =1, 2 and 3) (see Eq. (13)) into $D = 0$, we have

$$U_1 S^2\theta_3 + U_2 S\theta_3 + U_3 = 0 \tag{15}$$

where

$$\begin{cases} U_1 = l_3^2 S^2\alpha_2 \\ U_2 = 2l_3(d_3 + d_4)S\alpha_2 C\alpha_2 \\ U_3 = -l_3^2 - (d_3 + d_4)^2 S^2\alpha_2 \end{cases} \tag{16}$$

If no solution for θ_3 is obtained from Eq. (16), then the DSPB6RCT does not undergo self-motion that θ_2 can take any value. Otherwise, substitute each value for θ_3 obtained by solving Eq. (16) into Eq. (9) and solve the resulted equation for θ_1. If there is solution for θ_1, then the DSPB6RCT undergoes self-motion for the given set of θ_3 and θ_1. Otherwise, the DSPB6RCT does not undergo self-motion that θ_2 can take any value.

6. Numerical Examples

In this section, four numerical examples will be presented to verify the analytical solutions (Eqs. (12), (14) and (2)) to kinematic analysis of DSPB6RCTs and to show DSPB6RCTs with different number of circuits (closure modes) and different number of full-turn R joints. In addition, self-motion, if any, of DSPB6RCTs will also be investigated.

Considering the existence criteria (Eqs. (1) and (11)) of the DSPB6RCTs, one only needs to list the following link parameters that satisfy Eq. (11) for the example mechanisms: α_1, α_2, l_1, l_2, l_3, l_6, d_1, d_2, d_3, d_4, and d_6. In each mechanism, joint 3 is actuated. Link 3 is the frame of a DSPB6RCT, which is highlighted in the following CAD models of the DSPB6RCT in sample configurations.

6.1. DSPB6RCT 1

The link parameters of DSPB6RCT 1 are:

$\alpha_1 = -\pi/2$, $\alpha_2 = \pi/2$, $l_1 = -28.28$, $l_2 = 30.31$, $l_3 = 25$, $l_6 = 5\sqrt{265}$, $d_1 = -30$, $d_2 = 45.78$, $d_3 = -30$, $d_4 = -50$, and $d_6 = 50$.

The variation of θ_1 and θ_2 with θ_3 for DSPB6RCT 1 is obtained and shown in Fig. 4. Figure 4 shows that DSPB6RCT 1 has two circuits and two full-turn R joints (joints 3 and 4). Several sample configurations of the 6R mechanism on different circuits, configurations A to D on circuit 1 and configurations E to H on circuit 2, are shown in Fig. 5.

Now let us discuss whether DSPB6RCT 1 can undergo self-motion. For this DSPB6RCT, Eq. (15) becomes

$$25(25S^2\theta_3 - 281) = 0 \tag{17}$$

Solving Eq. (17), no solution to θ_3 is obtained. Therefore, the DSPB6RCT cannot undergo self-motion with θ_2 being of any value.

6.2. DSPB6RCT 2

The link parameters of DSPB6RCT 2 are:

$\alpha_1 = -\pi/4$, $\alpha_2 = -\pi/4$, $l_1 = l_2 = 0$, $l_3 = 50$, $l_6 = 50\sqrt{2}$, $d_1 = -50$, $d_2 = 20$, $d_3 = d_4 = 25$, and $d_6 = 50$.

The variation of θ_1 and θ_2 with θ_3 for DSPB6RCT 2 is obtained and shown in Fig. 6. Figure 6 shows that DSPB6RCT 2 has one circuit and no full-turn R joint. Configurations A, B and C indicated in Fig. 6 are shown in Fig. 7.

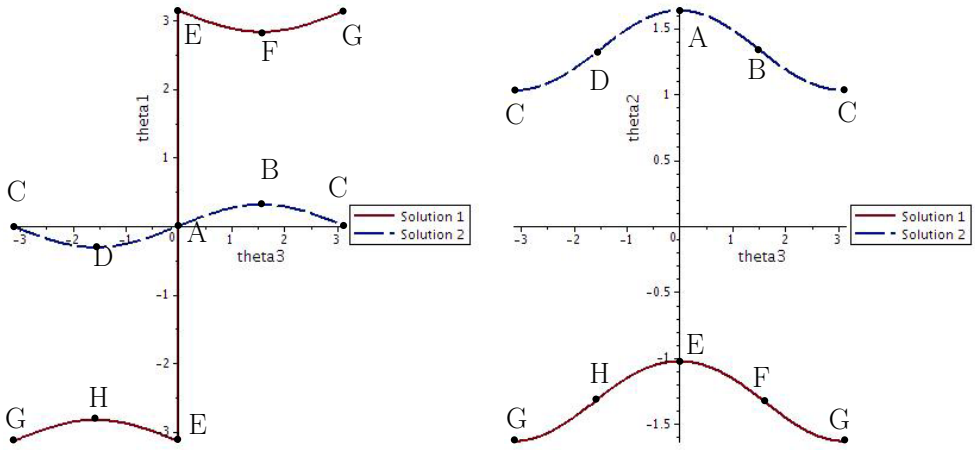

(a) Plot of θ_1-θ_3. (b) Plot of θ_2-θ_3.

Figure 4: Kinematic analysis of DSPB6RCT 1 ($\theta_6 = -\theta_1$, $\theta_5 = -\theta_2$ and $\theta_4 = -\theta_3$): Case with two circuits.

Now let us discuss whether DSPB6RCT 2 can undergo self-motion. For this DSPB6RCT, Eq. (15) becomes

$$1250(S^2\theta_3 - 2S\theta_3 - 3) = 0 \tag{18}$$

Solving Eq. (18), we obtain $\theta_3 = -\pi/2$. Under $\theta_3 = -\pi/2$, Eq. (9) is reduced to

$$\begin{cases} 50\sqrt{2}C\theta_1 = 0 \\ -50S\theta_1 = 0 \\ 50(\sqrt{2} - S\theta_1) = 0 \end{cases} \tag{19}$$

i.e.

$$\begin{cases} C\theta_1 = 0 \\ S\theta_1 = 0 \\ S\theta_1 = \sqrt{2} \end{cases} \tag{20}$$

From Eq. (20), no solution to θ_1 can be obtained. Therefore, the DSPB6RCT cannot undergo self-motion with θ_2 being of any value.

6.3. DSPB6RCT 3

The link parameters of DSPB6RCT 3 are:

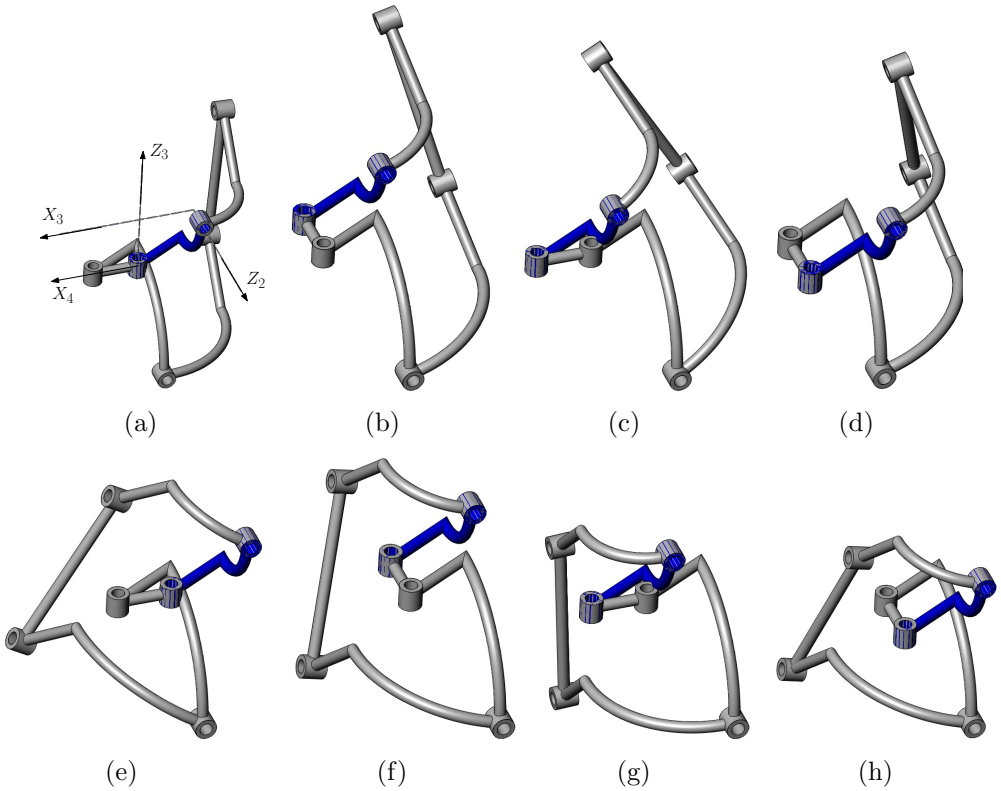

Figure 5: Configurations of DSPB6RCT 1: (a) Configuration A, (b) Configuration B, (c) Configuration C, (d) Configuration D, (e) Configuration E, (f) Configuration F, (g) Configuration G, and (h) Configuration H.

$\alpha_1 = \pi/2$, $\alpha_2 = -\pi/4$, $l_1 = 50$, $l_2 = 0$, $l_3 = 50$, $l_6 = 50$, $d_1 = -25$, $d_2 = 25$, $d_3 = d_4 = 0$, and $d_6 = 25$.

The variation of θ_1 and θ_2 with θ_3 for DSPB6RCT 3 is obtained and shown in Fig. 8. Figure 8 shows that DSPB6RCT 3 has two circuits and four full-turn R joints (joints 2, 3, 4 and 5). Configurations A and B on different circuits as indicated in Fig. 8 are shown in Fig. 9. In addition to circular translation, a DSPB6RCT with four full-turn R joints can also be used as a coupling connecting two non-parallel shafts.

Now let us discuss whether DSPB6RCT 3 can undergo self-motion. For this DSPB6RCT, Eq. (15) becomes

$$1250(S^2\theta_3 - 2) = 0 \tag{21}$$

Solving Eq. (21), no solution to θ_3 is obtained. Therefore, the DSPB6RCT

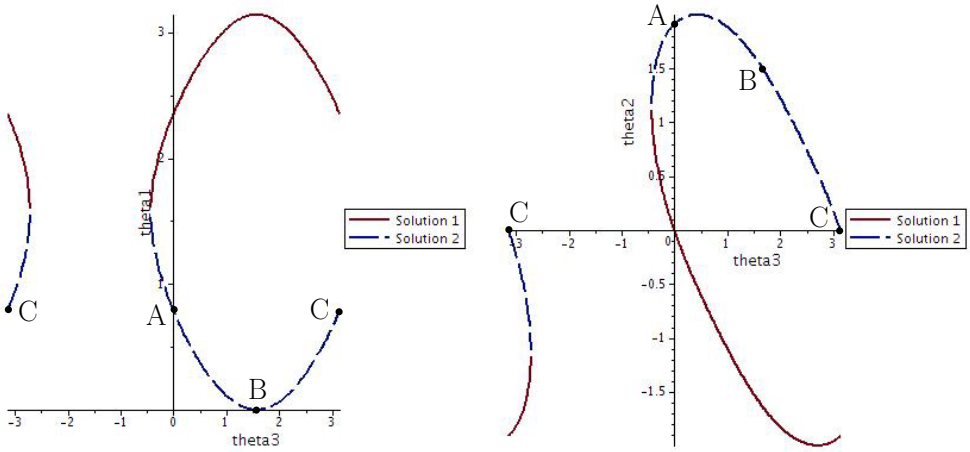

(a) Plot of θ_1-θ_3. (b) Plot of θ_2-θ_3.

Figure 6: Kinematic analysis of DSPB6RCT 2 ($\theta_6 = -\theta_1$, $\theta_5 = -\theta_2$ and $\theta_4 = -\theta_3$): Case with one circuit.

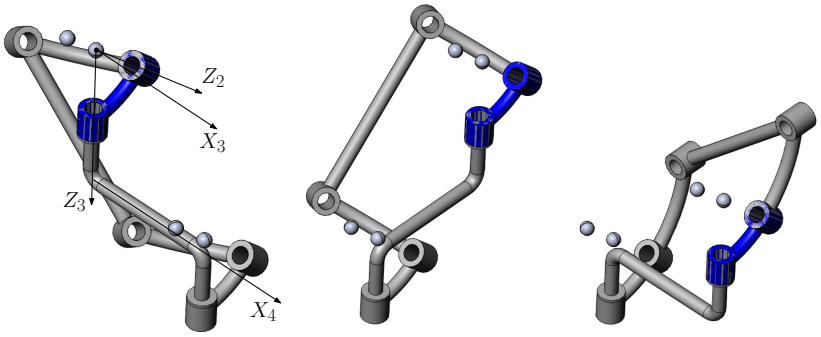

(a) Configuration A. (b) Configuration B. (c) Configuration C.

Figure 7: Configurations of DSPB6RCT 2.

cannot undergo self-motion with θ_2 being of any value.

6.4. DSPB6RCT 4

The link parameters of DSPB6RCT 4 are:

$\alpha_1 = -\pi/2$, $\alpha_2 = -\pi/4$, $l_1 = l_2 = 0$, $l_3 = 50$, $l_6 = 50\sqrt{2}$, $d_1 = -50$, $d_2 = 20$, $d_3 = d_4 = 25$, and $d_6 = 50$.

The variation of θ_1 and θ_2 with θ_3 for DSPB6RCT 4 is obtained and shown in Fig. 10. Figure 10 shows that DSPB6RCT 4 has one circuit (A-B-

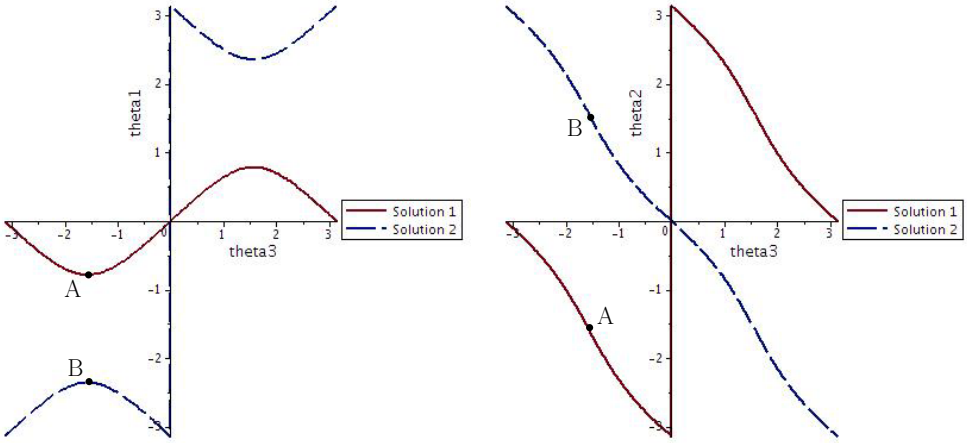

(a) Plot of θ_1-θ_3. (b) Plot of θ_2-θ_3.

Figure 8: Kinematic analysis of DSPB6RCT 3 ($\theta_6 = -\theta_1$, $\theta_5 = -\theta_2$ and $\theta_4 = -\theta_3$): Case with two circuits.

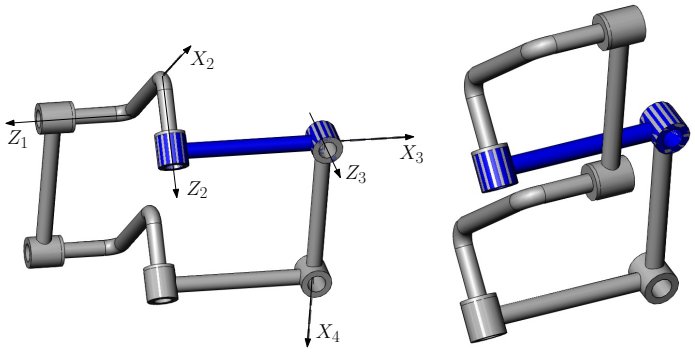

(a) Configuration A. (b) Configuration B.

Figure 9: Configurations of DSPB6RCT 3.

C-D-E-F-G-H-A) with a period of 4π in θ_3 and θ_4. Configurations A to H indicated in Fig. 10 are shown in Fig. 11.

Now let us discuss whether DSPB6RCT 4 can undergo self-motion. For this DSPB6RCT, Eq. (15) becomes

$$1250(S^2\theta_3 - 2S\theta_3 - 3) = 0 \tag{22}$$

Solving Eq. (22), we obtain $\theta_3 = -\pi/2$. Under $\theta_3 = -\pi/2$, Eq. (9) is

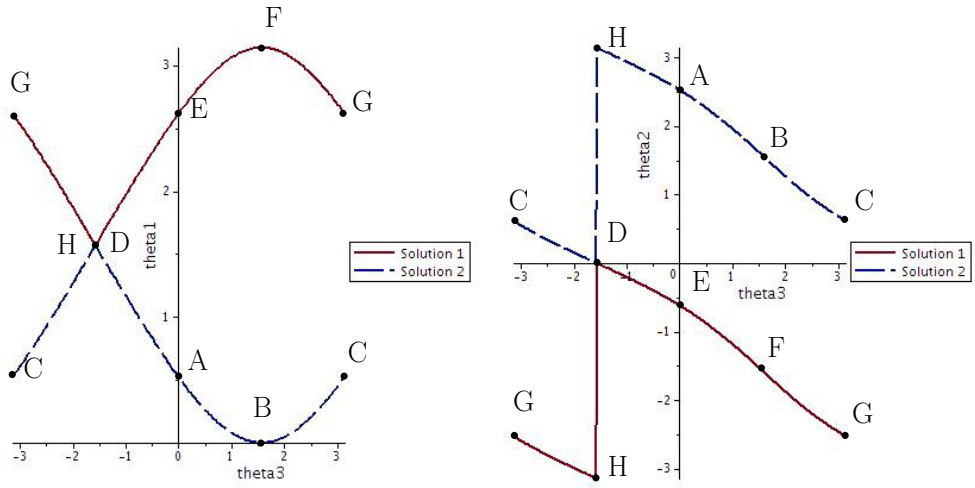

(a) Plot of θ_1-θ_3. (b) Plot of θ_2-θ_3.

Figure 10: Kinematic analysis of DSPB6RCT 4 ($\theta_6 = -\theta_1$, $\theta_5 = -\theta_2$ and $\theta_4 = -\theta_3$): Case with one circuit.

reduced to

$$\begin{cases} 50\sqrt{2}C\theta_1 = 0 \\ 0 = 0 \\ 50\sqrt{2}(S\theta_1 - 1) = 0 \end{cases} \tag{23}$$

i.e.

$$\begin{cases} C\theta_1 = 0 \\ S\theta_1 = 1 \end{cases} \tag{24}$$

From Eq. (24), we obtain $\theta_1 = \pi/2$.

Therefore, if $\theta_3 = -\pi/2$ and $\theta_1 = \pi/2$, Eq. (9) is satisfied for any value of θ_2. The DSPB6RCT can undergo self-motion with θ_2 being of any value. During the self-motion, the axes of joints 2 and 5 are collinear, links 5, 6 and 1 can rotate freely about the axes of joints 2 and 5 while the joint angles of the remaining four joints remain constant.

It is noted that two configurations, D and H, shown in Fig. 11 are also connected by the above self-motion (rotation about the axes of joints 2 and 5) in addition to the circuit A-B-C-D-E-F-G-H-A.

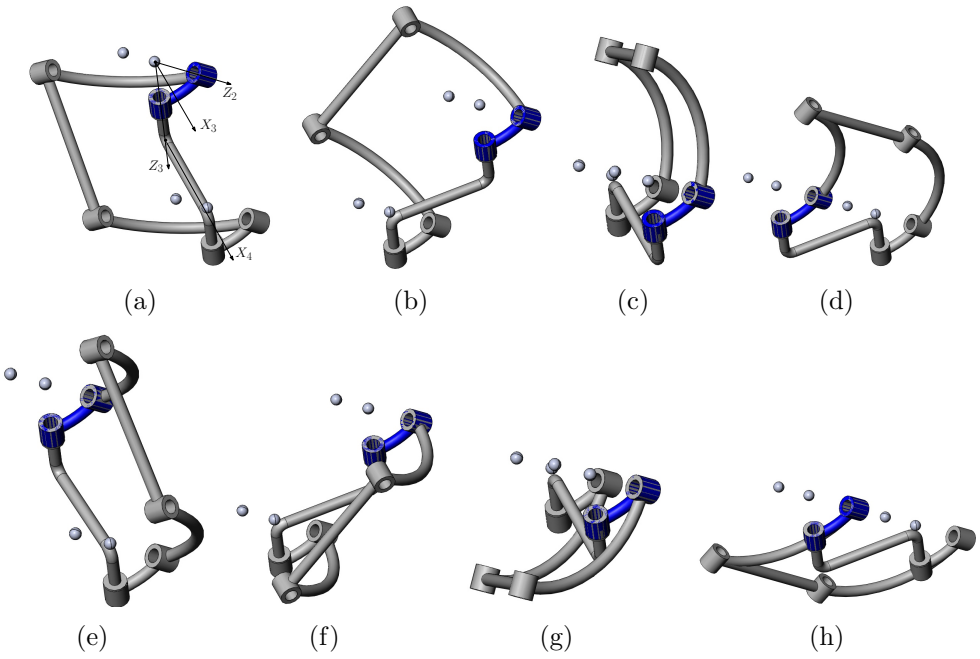

Figure 11: Configurations of DSPB6RCT 4: (a) Configuration A, (b) Configuration B, (c) Configuration C, (d) Configuration D, (e) Configuration E, (f) Configuration F, (g) Configuration G, and (h) Configuration H.

7. Conclusions

A closed-form solution has been derived for the DSPB6RCT. It has been shown that there are usually two solutions to the kinematic analysis for a given input and that a DSPB6RCT may have one or two circuits and 0, 2 or 4 full-turn R joints. The self-motion, if any, of the DSPB6RCTs has also been derived.

This work provides a solid starting point for further investigation on the classification and application of the DSPB6RCTs for circular translation or as a coupling connecting two non-parallel shafts as well as the kinematic analysis of other classes of overconstrained 6R spatial mechanisms for circular translation. The results can also be used for the type synthesis and singularity analysis of translational parallel mechanisms. It is still open to identify DSPB6RCTs that also satisfy the existence criteria of other classes of overconstrained mechanisms, which may have more than two circuits, as potential disassembly-free reconfigurable mechanisms.

References

[1] K.J. Waldron, Hybrid overconstrained linkages, *Journal of Mechanisms* 2 (1968) 73–78.

[2] J.E. Baker, The Bennett, Goldberg and Myard linkages - in perspective, *Mechanism and Machine Theory* 14 (1979) 239–253.

[3] C. Mavroidis and B. Roth, Analysis of overconstrained mechanism, *ASME Journal of Mechanical Design*, 117 (1995) 69–74.

[4] P. Dietmaier, A new 6R space mechanism, in: *Proceedings of the 9th World Congress IFToMM*, Milano, 1995, Vol. 1, pp. 52–56.

[5] K. Wohlhart, Merging two general Goldberg 5R linkages to obtain a new 6R space mechanism, *Mechanism and Machine Theory* 26 (2) (1991) 659–668.

[6] Six, K., and Kecskeméthy, A., "Steering properties of a combined wheeled and legged striding excavator," *Proceedings of the 10th World Congress on the Theory of Machines and Mechanisms*, Oulu, Finland, June 20-24, 1999, vol. 1, pp. 135-140.

[7] Zsombor-Murray, P.J., and Gfrerrer, A., "'Robotrac' mobile 6R closed chain," *Proceedings of CSME Forum 2002*, ISBN 0-9730900, Kingston, Canada, May 21-24, 2002, Paper number, 02-05

[8] J.E. Baker, A curious new family of overconstrained six-bars, *ASME Journal of Mechanical Design*, **127**(4) (2005) 602–606.

[9] Y. Chen and Z. You, An extended Myard linkage and its derived 6R linkage, *ASME Journal of Mechanical Design*, 130(5) (2008) 052301.

[10] J.E. Baker, Using the single reciprocal screw to confirm mobility of a six-revolute linkage, *Proceedings of the Institution of Mechanical Engineers. Part C: Journal of Mechanical Engineering Science* **224**(10) (2010) 2247-2255.

[11] M. Pfurner, A new family of overconstrained 6R-mechanisms, *Proceedings of EUCOMES 08*, M. Ceccarelli (Ed), Springer Netherlands, 2009, pp. 117–124.

[12] J.M. Hervé, A new four-bar linkage completing Delassus findings, *Transactions of the Canadian Society for Mechanical Engineering*, **35** (1) (2011) 57–62

[13] G. Hegedüs, J. Schicho, and H.-P. Schröcker,, Construction of overconstrained linkages by factorization of rational motions, Latest Advances in Robot Kinematics, J. Lenarčič, M. Husty (Eds.), Springer Netherlands, 2012, pp. 213-220.

[14] Z. Li, and J. Schicho, Classification of angle-symmetric 6R linkages, *Mechanism and Machine Theory* **70** (2013) 372–379.

[15] Z. Li, and J. Schicho, "Three types of parallel 6R linkages," *Computational Kinematics*, F. Thomas A. and Perez Gracia (Eds), Springer Netherlands, 2014, pp. 111–119.

[16] X. Kong, Type synthesis of single-loop overconstrained 6R mechanisms for circular translation, ASME J of Mechanisms and Robotics (2014) 6(4): 041016.

[17] C.-C. Lee and H.-S. Yan, "Movable spatial 6R mechanisms with three adjacent parallel axes," *ASME Journal of Mechanical Design*, 115(3), (1993) pp. 522–529.

[18] J.E. Baker, 2003. "Overconstrained six-bars with parallel adjacent joint-axes," *Mechanism and Machine Theory*, **38**(2), pp. 103-117.

[19] Q. Jin, and T.-L. Yang, Overconstraint analysis on spatial 6-link loops, *Mechanism and Machine Theory* **37**(3) (2002) 267–278.

[20] J.E. Baker, Displacement-closure equations of the unspecialised double-Hookes-joint linkage, *Mechanism and Machine Theory*, **37**(10) (2002) 1127-1144.

[21] L. Cui, and J.S. Dai, Axis constraint analysis and its resultant 6R double-centered overconstrained mechanisms, *Journal of Mechanisms and Robotics*, **3**(3) (2011) 031004.

[22] C.C. Lee, Analysis and synthesis of Schatz six-revolute mechanisms, *JSME International Journal*, Series C **43**(1) (2000) 80–91.

[23] W.W. Gan, S. Pellegrino, A numerical approach to the kinematic analysis of deployable structures forming a closed loop, Proceedings of the Institution of Mechanical Engineers, Part C: Journal of Mechanical Engineering Science 220 (2006) 10451056.

[24] C. Galletti, P. Fanghella, Single-loop kinematotropic mechanisms, Mechanism and Machine Theory 36 (2001) 743–761.

[25] C.C. Lee, J.M. Hervé, Discontinuously movable seven-link mechanisms via group-algebraic approach, Proceedings of the Institution of Mechanical Engineers, Part C: Journal of Mechanical Engineering Science 219 (2005) 577–587.

[26] X. Kong, C. Huang, Type synthesis of single-DOF single-loop mechanisms with two operation modes, *Proceedings of the 2009 ASME/IFToMM International Conference on Reconfigurable Mechanisms and Robots*, London, UK, 2009, pp. 136–141.

[27] K. Wohlhart, Multifunctional 7R linkages, *Proceedings of the International Symposium on Mechanisms and Machine Theory*, AzCIFToMM, Izmir, Turkey, 2010, pp. 85–91.

[28] C.Y. Song, Y. Chen, and I-M. Chen, A 6R linkage reconfigurable between the line-symmetric Bricard linkage and the Bennett linkage, *Mechanism and Machine Theory* **70** (2013) 278–292.

[29] X. Kong, and M. Pfurner, Type synthesis and reconfiguration analysis of variable-DOF single-loop mechanisms, *Mechanism and Machine Theory*, **85** (2015) 116-128.

[30] X. Kong, and C.M. Gosselin, Type synthesis of three-degree-of-freedom spherical parallel manipulators, *International Journal of Robotics Research* **23**(3) (2004) 237–245.

[31] L. Kronig, Overview of biomimetics and artiomemetics in robotics, Final Year Undergraduate Project Report, Heriot-Watt University, Edinburgh, UK, 2010.

[32] X. Kong, and Y. Jin, Type Synthesis of 3-DOF multi-mode translational/spherical parallel mechanisms with

lockable joints, *Mechanism and Machine Theory* (2015) http://dx.doi.org/10.1016/j.mechmachtheory.2015.04.019

[33] L. Racila, M. Dahan, Spatial properties of Wohlhart symmetric mechanism, Meccanica 45 (2010) 153-165.

[34] C.C. Lee and J.M. Hervé, "Geometric derivation of 6R linkages with circular translation," *Advances in Robot Kinematics*, J. Lenarčič and O. Khatib (Eds), Springer, Netherlands, 2014, pp. 59–67.

[35] X. Kong, and C. Gosselin, 2007, *Type Synthesis of Parallel Mechanisms*, Springer, New York.

[36] H. Lipkin, "A note on Denavit-Hartenberg notation in robotics," *Proceedings of the ASME 2005 International Design Engineering Technical Conferences & Computers and Information in Engineering Conference*. September 24-28, 2005, Long Beach, California, USA, DETC2005-85460.

[37] D. Chablat, Ph. Wenger and I. Bonev, Self motions of a special 3-RPR planar parallel robot, *Advances in Robot Kinematics*, J. Lenarčič and B. Roth (eds.), 2006, pp. 221-228.

[38] X. Kong, Forward displacement analysis of a 3-RPR planar parallel manipulator revisited, *Computational Kinematics*, A. Kecskeméthy and A. Müller (Eds), Springer, 2009, pp. 69–76.